

## Supplementary information

### Metal-Organic Frameworks (MOFs) as highly efficient agents for boron removal and boron isotopes separation

Jiafei Lyu, Hongxu Liu, Jingshuang Zhang, Zhouliangzi Zeng, Peng Bai, Xianghai Guo\*

\*Corresponding Author: Xianghai Guo

Fax: 86-22-27406186

Email: guoxh@tju.edu.cn

## **Contents**

**Section S1. Research on boron isotopes separation with boron adsorbents**

**Section S2. Summary of boron adsorbents.**

**Section S3. Characterization of ZIF-8**

**Section S4. Characterization of UiO-66**

**Section S5. Characterization of MIL-100(Fe)**

**Section S6. Characterization of MIL-101(Cr)**

**Section S7. Characterization of MIL-100(Cr)**

**Section S8. Characterization of MIL-53(Cr)**

**Section S9. Characterization of MIL-96(Al)**

**Section S10. Calculation of separation factor and adsorption capacity**

**Section S11. Boron concentration and isotopic abundance of residual boron aqueous solutions**

**Section S12. Boron adsorption mechanism**

**Section S13. References**

## Section S1. Research on boron isotopes separation with boron adsorbents

**Table S1** Research on boron isotopes separation with boron adsorbents.

Adsorbents	Temperature (°C)	pH	Boron concentration (mmol·L <sup>-1</sup> )	Isotopes separation factor, S	Refs
<b>Strongly basic anion exchange resin</b>					
Amberlite CG-400I	R. T.	Not mention	100 <sup>a</sup>	1.016	1
Diaion PA-312	25	>12 <sup>b</sup>	10.4	1.019	2
Diaion SA-20A	25	12 <sup>b</sup>	106	1.011	2
<b>Weakly basic anion exchange resin</b>					
Diaion WA-21	5	10.5-11 <sup>b</sup>	10.4	1.023	2
Diaion WA-10	25	11-11.5 <sup>b</sup>	10.1	1.016	2
Diaion WA 30	25	11.5 <sup>b</sup>	9.99	1.017	2
Muromac 1×8	25	neutral	0.10	1.018	3
Muromac 1×8	25	neutral	0.10	1.012	3
<b>Boron-selective resin</b>					
CRB-02	25(50)	Not mention	100	1.018-1.022	4
<i>N</i> -Methyl-D-					
Glucamine Type Resin	Not mention	<7	100 <sup>c</sup>	1.027	5
<b>Clay</b>					
Kaolin	20	5	10.10	1.0023	6
Kaolin	25	5	9.51	1.0011	7
<b>Other adsorbents</b>					
Mg(OH) <sub>2</sub>	25	10.5	45.9 <sup>c</sup>	1.022	8
Humic acids	25	5	3	1.027	9

<sup>a</sup> containing 8 wt. % purified glycerol.

<sup>b</sup> pH of the resin phase.

## Section S2. Summary of boron adsorbents.

**Table S2** Summary of boron adsorbents.

Adsorbents	Temperature (°C)	pH	Residual boron concentration (mmol·L⁻¹)	Adsorption capacity (mmol·g⁻¹)	Refs
<b>Cheleating resins</b>					
Amberlite IRA-743	25	7.0	8.00	0.71	<sup>10</sup>
Pyrocatechol modified resin	25	9.0	2.00	0.42	<sup>11</sup>
poly( <i>N</i> -(4-vinylbenzyl)- <i>N</i> -methyl- <i>D</i> -glucamine) (P(VbNMDG))	25	-	1.850 <sup>a</sup>	98% <sup>b</sup>	<sup>12</sup>
<b>Industrial waste</b>					
Fly ash	25	10-11	1.00 <sup>a</sup>	94% <sup>b</sup>	<sup>13</sup>
Palm oil mill boiler bottom ash	25	8.0	1.20	0.0435	<sup>14</sup>
Calcined magnesite tailing	45	6.0	50.90	6.1	<sup>15</sup>
<b>Natural materials</b>					
Calcined Alunite	25	10.0	16.70	0.31	<sup>16</sup>
Calcium alginate gel	25	9-10	18.50 <sup>a</sup>	94	<sup>17</sup>
Waste sepiolite	20	10	55.50 <sup>a</sup>	16.52	<sup>18</sup>
<b>New type inorganic sorbents</b>					
MG modified SBA-15	25	7-12	0.93 <sup>a</sup>	45% <sup>b</sup>	<sup>19</sup>
MG modified MCM-41	25	6	9.25×10 <sup>-4</sup> <sup>a</sup>	0.8	<sup>20</sup>
Mg/Al layered double hydroxide	25	10	46.07 <sup>a</sup>	90% <sup>b</sup>	<sup>21</sup>
Si-MG	25	7	0.20	1.54	<sup>22</sup>
ZIF-8	25	-	500 <sup>a</sup>	17.67	This study

<sup>a</sup> Initial boron concentrations (mmol·L⁻¹).

<sup>b</sup> boron recovery efficiency.

## Section S3. Characterization of ZIF-8

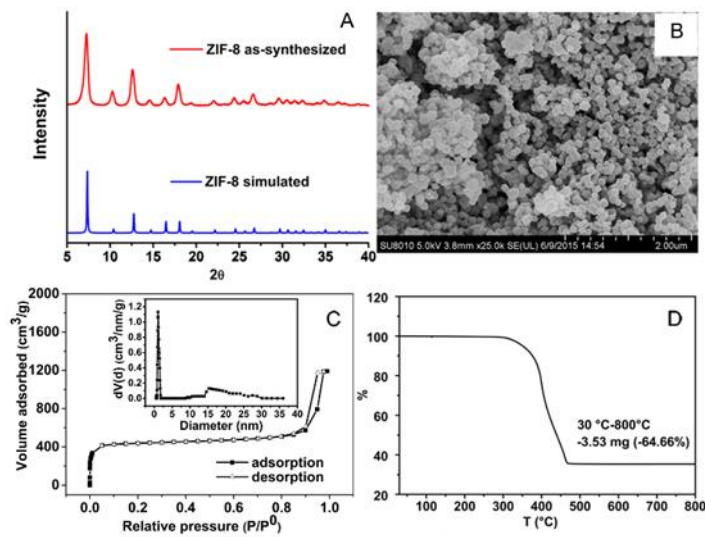


**Fig. S1.** Characterization of ZIF-8. a) XRD patterns; b) SEM image; c) N<sub>2</sub> adsorption/desorption isotherms and the pore size distribution (inset); d) TGA curve.

#### Section S4. Characterization of UiO-66

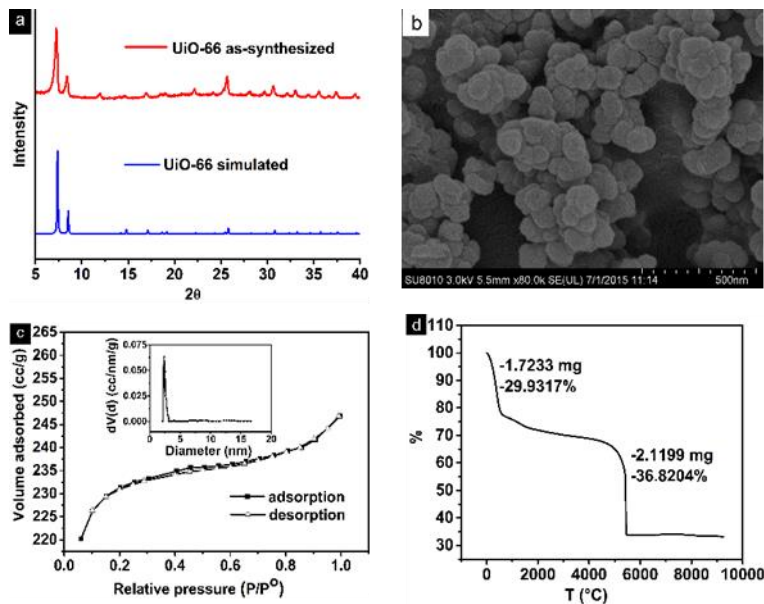


**Fig. S2.** Characterization of UiO-66. a) XRD patterns; b) SEM image; c) N<sub>2</sub> adsorption/desorption isotherms and the pore size distribution (inset); d) TGA curve.

#### Section S5. Characterization of MIL-100(Fe)

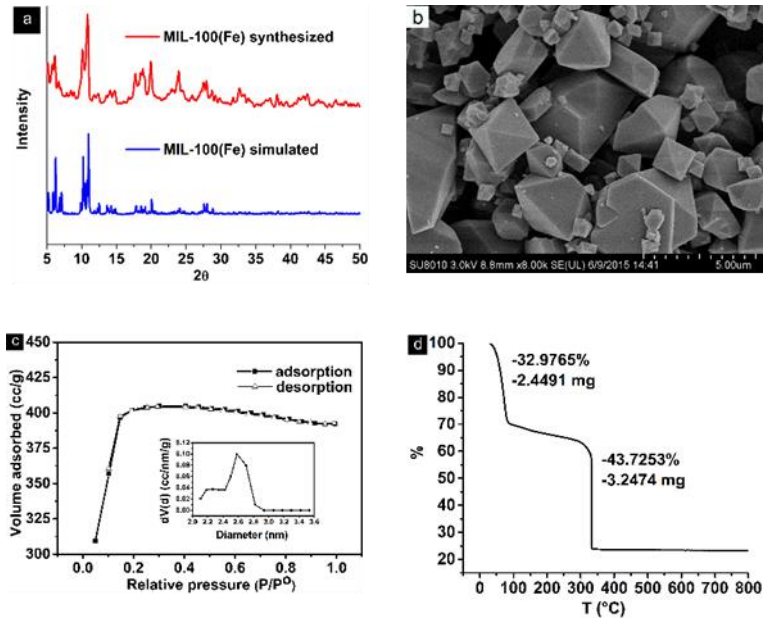


**Fig. S3.** Characterization of MIL-100(Fe). a) XRD patterns; b) SEM image; c)  $N_2$  adsorption/desorption isotherms and the pore size distribution (inset); d) TGA curve.

### Section S6. Characterization of MIL-101(Cr)

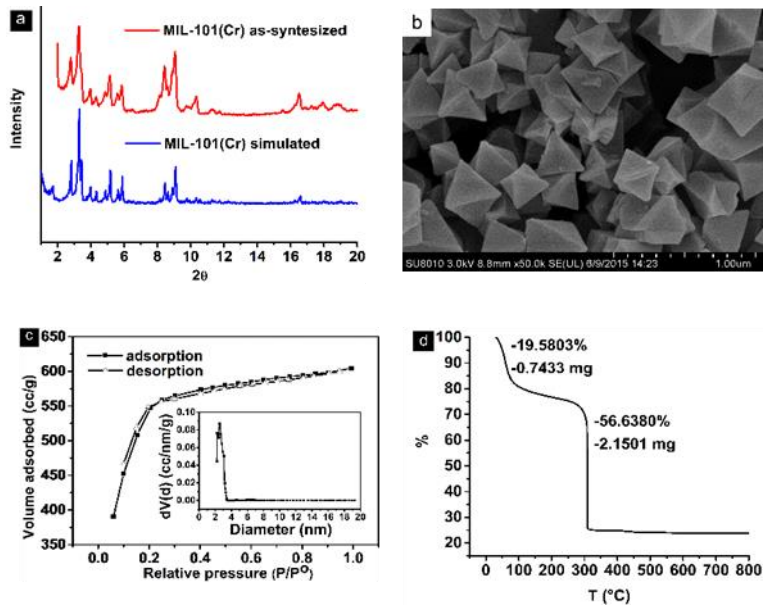


**Fig. S4.** Characterization of MIL-101(Cr). a) XRD patterns; b) SEM image; c)  $N_2$  adsorption/desorption isotherms and the pore size distribution (inset); d) TGA curve.

### Section S7. Characterization of MIL-100(Cr)

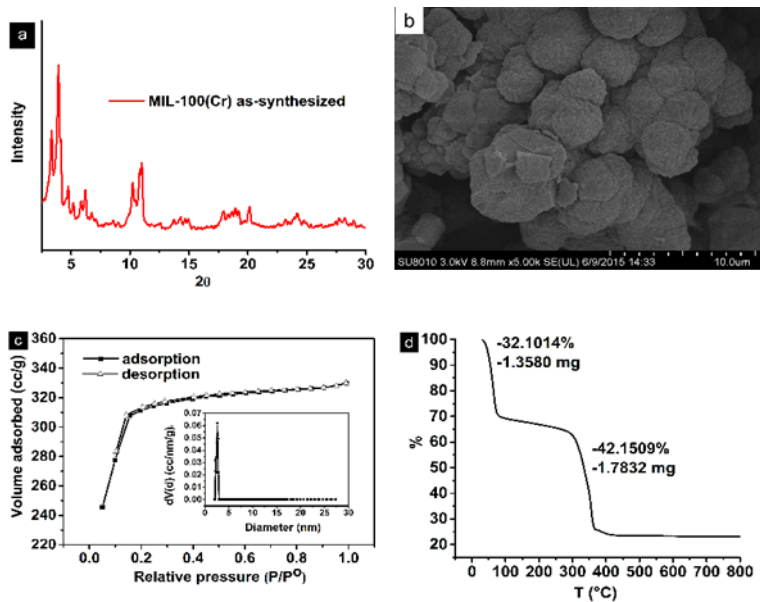


**Fig. S5.** Characterization of MIL-100(Cr). a) XRD patterns; b) SEM image; c)  $N_2$  adsorption/desorption isotherms and the pore size distribution (inset); d) TGA curve.

### Section S8. Characterization of MIL-53(Cr)

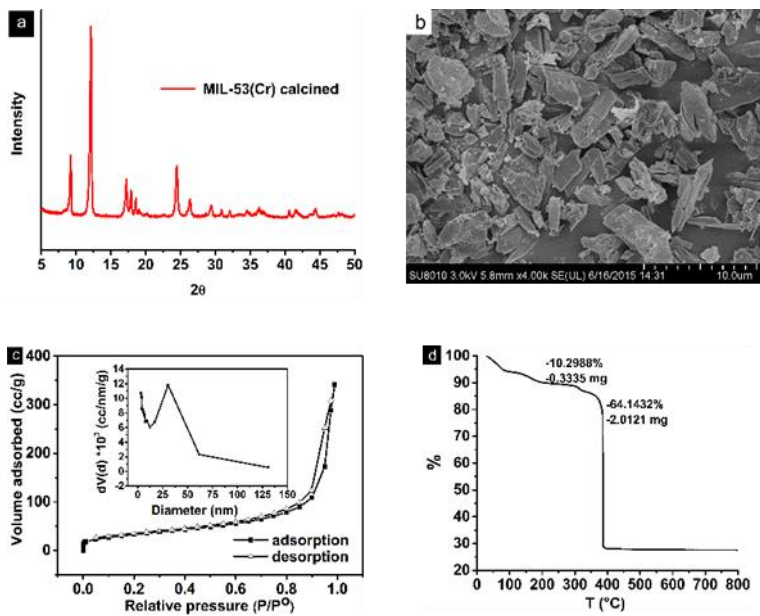


**Fig. S6.** Characterization of MIL-53(Cr). a) XRD patterns; b) SEM image; c)  $N_2$  adsorption/desorption isotherms and the pore size distribution (inset); d) TGA curve.

### Section S9. Characterization of MIL-96(Al)

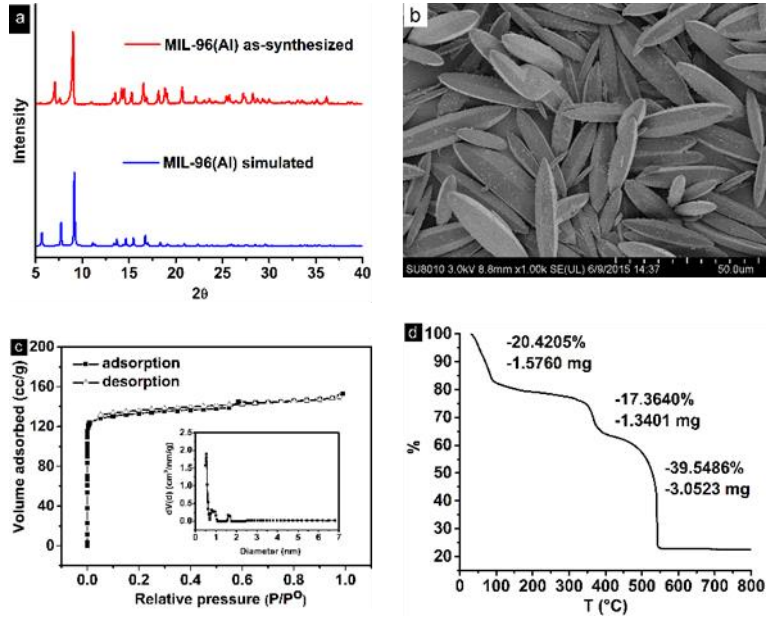


**Fig. S7.** Characterization of MIL-96(Al). a) XRD patterns; b) SEM image; c)  $N_2$  adsorption/desorption isotherms and the pore size distribution (inset); d) TGA curve.

### Section S10. Calculation of separation factor and adsorption capacity

The boron adsorption capacity  $Q$  ( $\text{mg}\cdot\text{g}^{-1}$ ) can be calculated based on the following equation:

$$Q = \frac{(c_0 - c_1)M}{D} \times 1000 \quad (1)$$

where  $c_0$  represents initial boron concentration,  $\text{mol}\cdot\text{L}^{-1}$ ;  $c_1$  represents residual boron concentration,  $\text{mol}\cdot\text{L}^{-1}$ ;  $M$  means the molecular weight of boron, 10.81  $\text{g}\cdot\text{mol}^{-1}$ ;  $D$  means the dosage of adsorbents, 5  $\text{g}\cdot\text{L}^{-1}$ .

The separation factor  $S$  can be calculated according to following equation:

$$\begin{aligned} S(\text{B}^{10}/\text{B}^{11}) &= \left[ \text{B}^{10}/\text{B}^{11} \right]_{\text{adsorbent}} / \left[ \text{B}^{10}/\text{B}^{11} \right]_{\text{solution}} \\ &= \left[ \left( c_0 \cdot \frac{\alpha_0}{\alpha_0 + 1} - c_1 \cdot \frac{\alpha_1}{\alpha_1 + 1} \right) / \left( c_0 \cdot \frac{1}{\alpha_0 + 1} - c_1 \cdot \frac{1}{\alpha_1 + 1} \right) \right] / \alpha_1 \\ &= \frac{c_0 \alpha_0 (1 + \alpha_1) - c_1 \alpha_1 (1 + \alpha_0)}{c_0 \alpha_1 (1 + \alpha_1) - c_1 \alpha_0 (1 + \alpha_0)} \end{aligned} \quad (2)$$

$$S(\text{B}^{11}/\text{B}^{10}) = \frac{1}{S(\text{B}^{10}/\text{B}^{11})} \quad (3)$$

where  $\alpha_0$  represents initial  $^{10}\text{B}/^{11}\text{B}$  abundance, 0.24779;  $\alpha_1$  represents  $^{10}\text{B}/^{11}\text{B}$  abundance of the residual solution.

### Section S11. Boron concentration and isotopic abundance of residual boron aqueous solutions

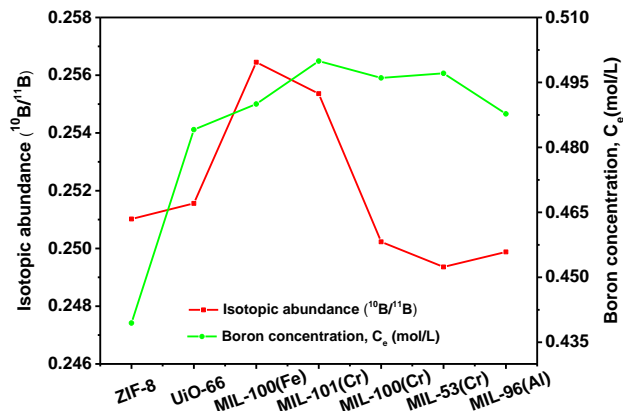


**Fig. S8.** boron concentration and isotopic abundance of residual boron aqueous solutions.

### Section S12. Boron adsorption mechanism on ZIF-8

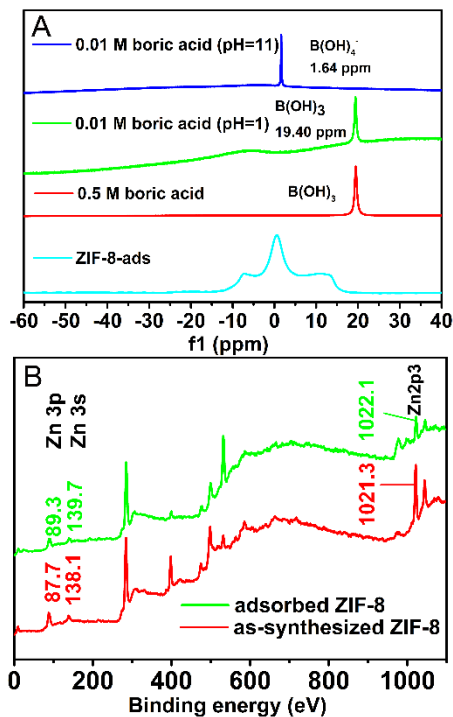


**Fig. S9** (A)  $^{11}\text{B}$  NMR of boric acid aqueous solutions and adsorbed ZIF-8; (B) XPS patterns of adsorbed and as-synthesized ZIF-8.

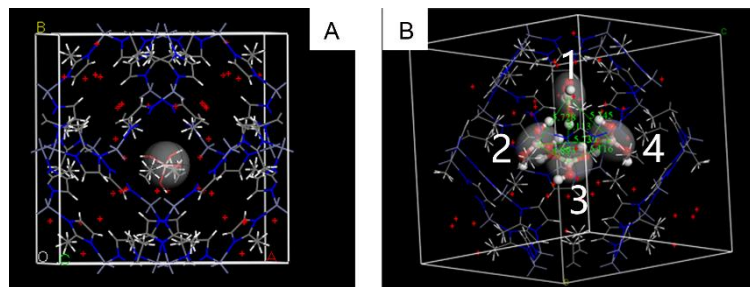


**Fig. S10** (A) Simulation of boron adsorption in the style of  $\text{B}(\text{OH})_4^-$  on ZIF-8; (B) Simulation of boron adsorption in the style of  $\text{B}(\text{OH})_3$  on ZIF-8. (Task: locate, Method: metropolis, Quality: customized, Force field: Universal).

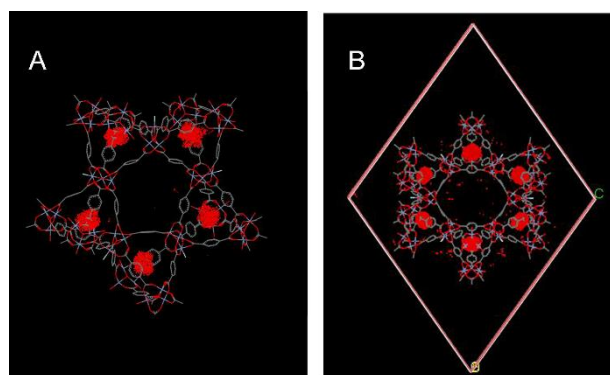


**Fig. S11** Simulation of boron adsorption in the style of  $\text{B}(\text{OH})_3$  on MIL-101(Cr). The red in the cages represents the adsorbed boric acid molecules. (A) pentagonal window; (B) hexagonal window. (Task: locate, Method: metropolis, Quality: customized, Force field: Universal).

### Section S13. References

1. T. U. Yokio Yoneda, Shoji Makishima, *The Journal of Physical Chemistry*, 1959, **63**, 2057-2058.
2. M. K. H. Kakihana, S. Satoh, M. Nomura, M. Okamoto, *Bull. Chem. Soc. Jpn.*, 1977, **50**, 158-163.
3. M. Musashi, T. Oi, M. Matsuo and M. Nomura, *Journal of Chromatography A*, 2008, **1201**, 48-53.
4. T. Oi, H. Shimazaki, R. Ishii and M. Hosoe, *Sep. Sci. Technol.*, 1997, **32**, 1821-1834.
5. Y. M. K. O. Akinari Sonoda, Norio Takagi, Takahiro Hirotsu, *Bulletin of the Chemical Society of Japan*, 2000, **73**, 1131-1133.
6. M. Musashi, M. Matsuo, T. Oi and Y. Fujii, *Geochemical Journal*, 2005, **39**, 105-111.
7. M. Musashi, M. Matsuo, T. Oi and M. Nomura, *Journal of Nuclear Science and Technology*, 2006, **43**, 461-467.

8. J. Xiao, Y. Xiao, C. Liu, Z. Zhao, M. He and C. Liang, *Chinese Science Bulletin*, 2009, **54**, 3090-3100.
9. E. Lemarchand, J. Schott and J. Gaillardet, *Geochim Cosmochim Ac*, 2005, **69**, 3519-3533.
10. Y. T. Wei, Y. M. Zheng and J. P. Chen, *Water Res*, 2011, **45**, 2297-2305.
11. B. Wang, H. Lin, X. Guo and P. Bai, *Desalination*, 2014, **347**, 138-143.
12. P. Santander, B. L. Rivas, B. F. Urbano, İ. Yılmaz İpek, G. Özkula, M. Arda, M. Yüksel, M. Bryjak, T. Kozlecki and N. Kabay, *Desalination*, 2013, **310**, 102-108.
13. S. Yüksel and Y. Yürüm, *Sep. Sci. Technol.*, 2009, **45**, 105-115.
14. M. F. Chong, K. P. Lee, H. J. Chieng and R. Syazwani Binti, ll, *Water Res*, 2009, **43**, 3326-3334.
15. I. Kipcak and M. Ozdemir, *Chem. Eng. J.*, 2012, **189**, 68-74.
16. D. Kavak, *J Hazard Mater*, 2009, **163**, 308-314.
17. M. Ruiz, C. Tobalina, H. Demey-Cedeño, J. A. Barron-Zambrano and A. M. Sastre, *Reactive and Functional Polymers*, 2013, **73**, 653-657.
18. D. K. N. Öztürk, *Adsorption*, 2004, **10**, 245-257.
19. T. Ben Amor, I. dhaouadi, B. Lebeau, M. Tlili and M. Ben Amor, *Desalination*, 2014, **351**, 82-87.
20. Ö. Kaftan, M. Açıkel, A. E. Eroğlu, T. Shahwan, L. Artok and C. Ni, *Anal Chim Acta*, 2005, **547**, 31-41.
21. M. Kurashina, T. Inoue, C. Tajima and E. Kanezaki, *Mod Phys Lett B*, 2015, **29**, 5.
22. L. Xu, Z. X. Miao, L. L. Fan and P. E. S. leee, *2012 Ieee Pes Transmission and Distribution Conference and Exposition (T&D)*, 2012.